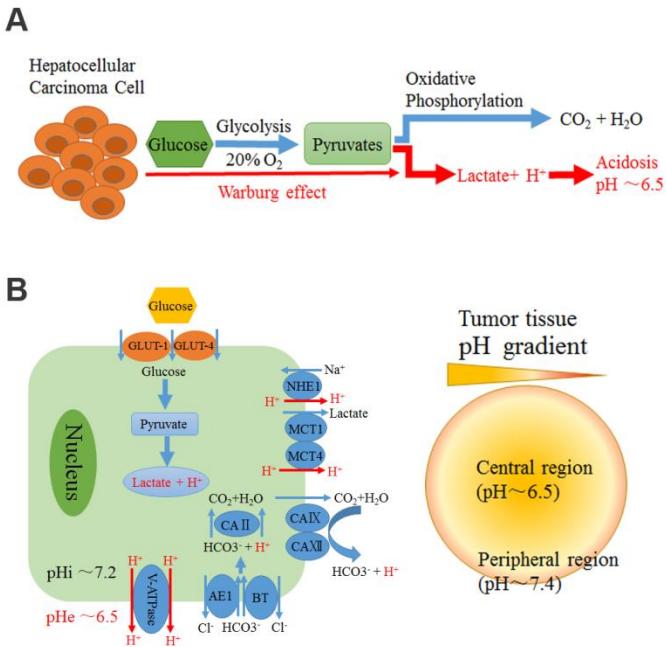
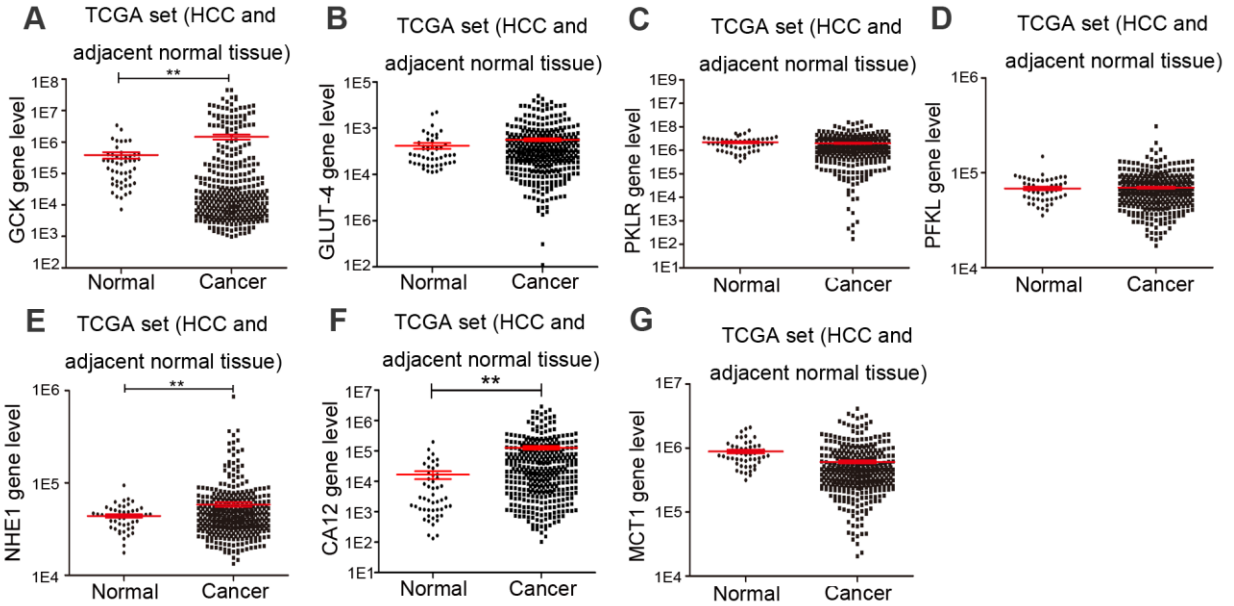


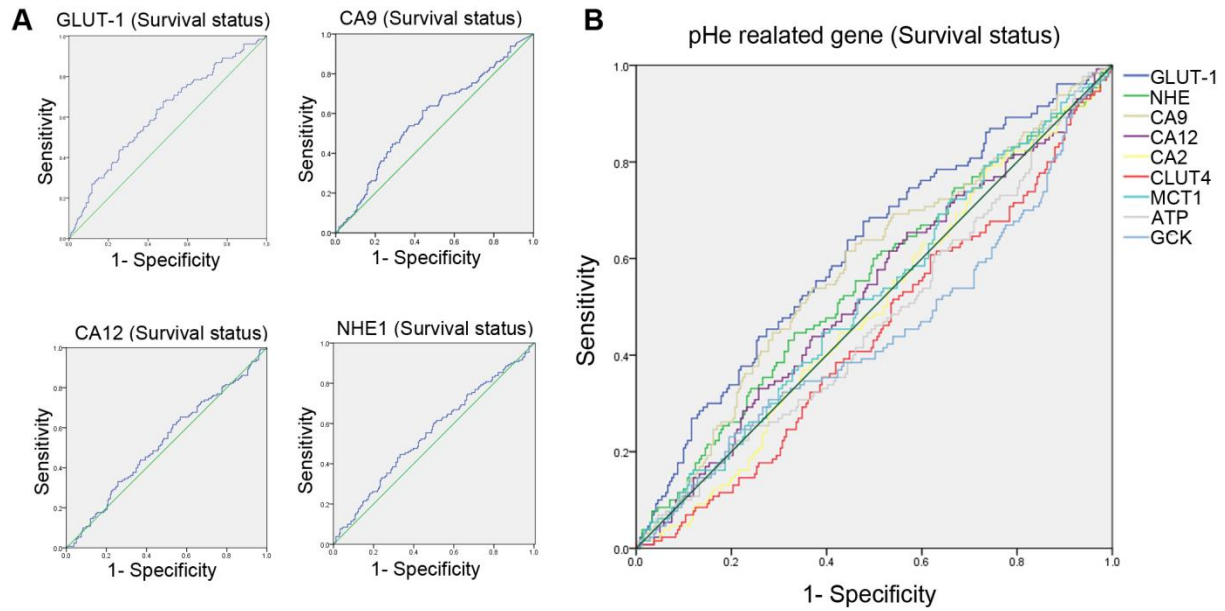
## Supplementary Figures and legends



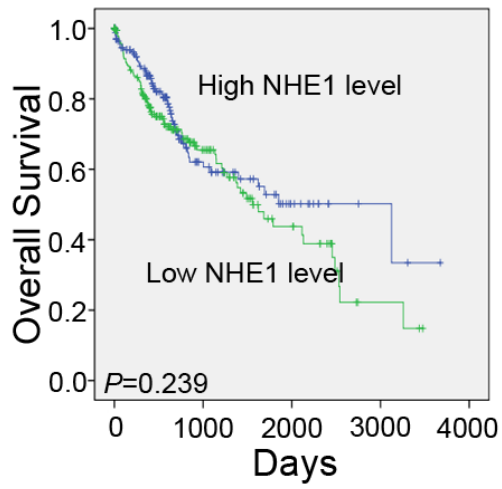
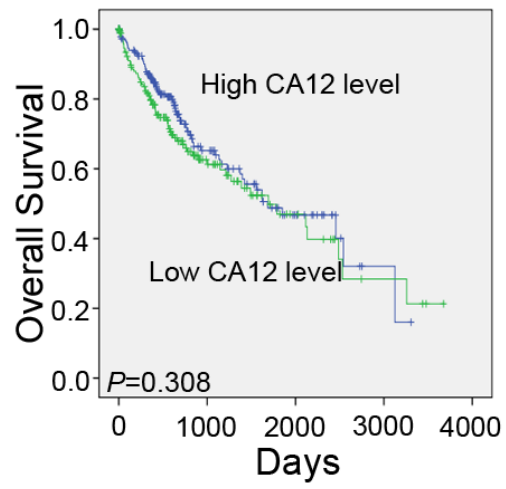
**Supplementary Figure S1.** Dysregulation of the pH gradient in and around cancer cells. **A.** Tumor cells cloned in both primary and early malignant lesions consume glucose at a high rate even in an oxygenated environment known as Warburg effect. **B.** Increased expression and activity of plasma membrane transporters maintain the high pH<sub>i</sub> and low pH<sub>e</sub> of HCC cells. **C.** Abnormal blood perfusion and hypoxia coupled with glycolytic phenotype generate pH gradient from the inner tumor region to adjacent normal tissue. MCT, monocarboxylate transporter; NHE1, Na<sup>+</sup>-H<sup>+</sup> exchanger 1. CA, carbonic anhydrase. AE1/BT, Cl<sup>-</sup>-HCO<sub>3</sub> exchanger.



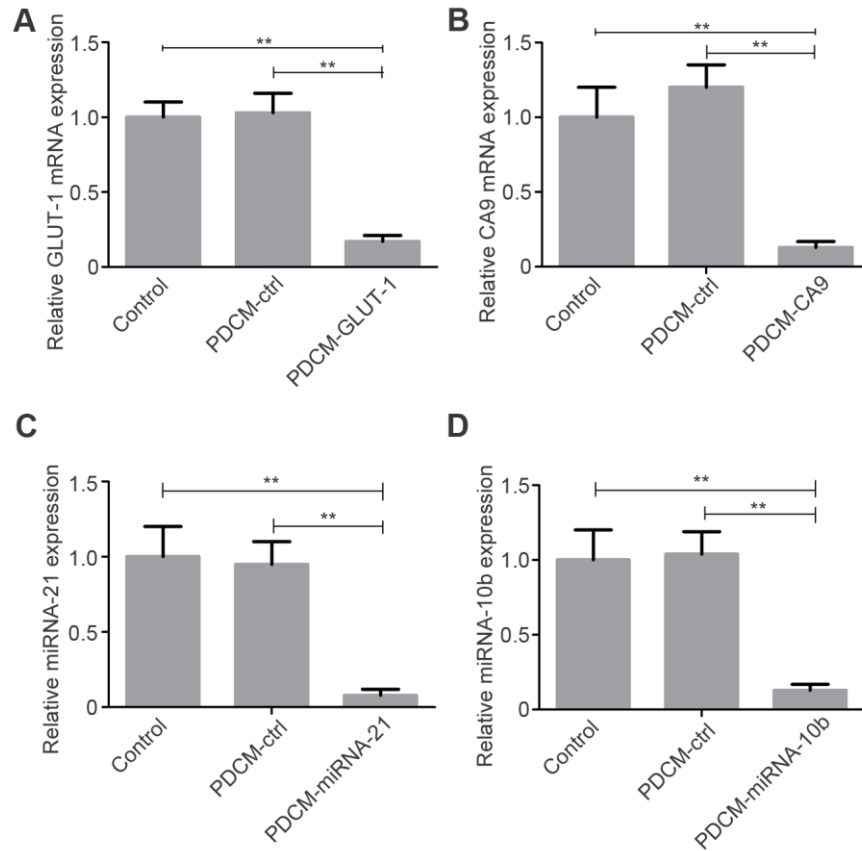
**Supplementary Figure S2. Expression levels of acidic pH-related genes in HCC tissues compared with adjacent normal tissues explored in the TCGA dataset.** A. *GCK*, B. *GLUT-4*, C. *PKLR*, D. *PFKL*, E. *NHE1*, F. *CA12*, G. *MCT1*. *GCK*, glucokinase. *GLUT-4*, solute carrier family 2 (facilitated glucose transporter), member 4. *PKLR*, pyruvate kinase L/R. *PFKL*, phosphofructokinase. *NHE1*,  $\text{Na}^+ - \text{H}^+$  exchanger 1. *CA12*, carbonic anhydrase 12. *MCT1*, monocarboxylate transporter 1.



**Supplementary Figure S3. ROC analysis shows the sensitivity and specificity of acidic pH-related genes and survival explored in TCGA dataset.** GLUT-1, solute carrier family 2 (facilitated glucose transporter), member 1. GLUT-4, solute carrier family 2 (facilitated glucose transporter), member 4. *PKLR*, pyruvate kinase L/R. *PFKL*, phosphofructokinase. *NHE1*,  $\text{Na}^+/\text{H}^+$  exchanger 1. *CA12*, carbonic anhydrase 12. *MCT1*, monocarboxylate transporter 1. *GCK*, glucokinase. *ATP*, V-ATPase.

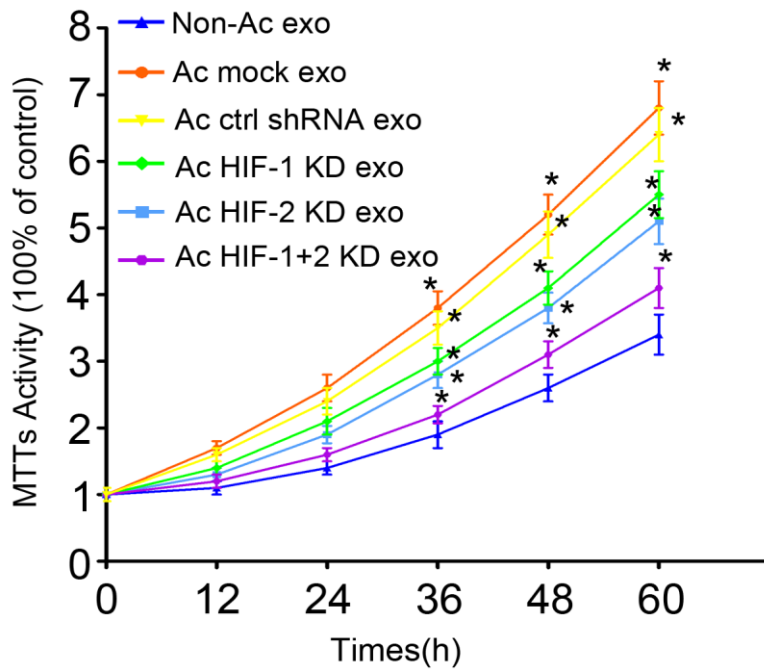
**A****B**

**Supplementary Figure S4. Kaplan-Meier analysis shows the correlation of GLUT-1/CA9 gene expression and poor overall survival in HCC patients explored in TCGA dataset. A. *NHE1*,  $\text{Na}^+/\text{H}^+$  exchanger 1. B. *CA12*, carbonic anhydrase 12.**

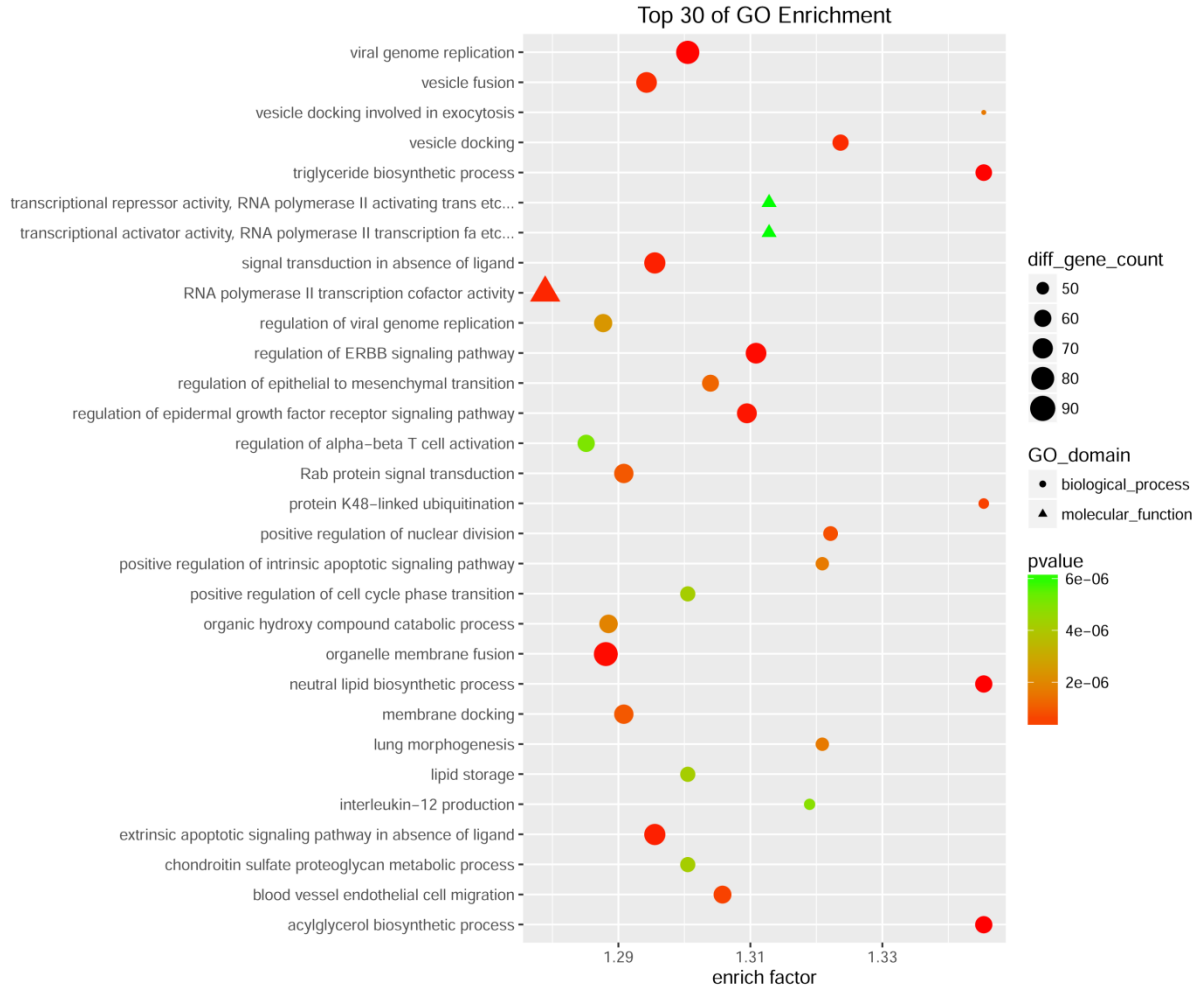


**Supplementary Figure S5. Real-time PCR validates the function of PDCM system in SMMC-7721 cells.**

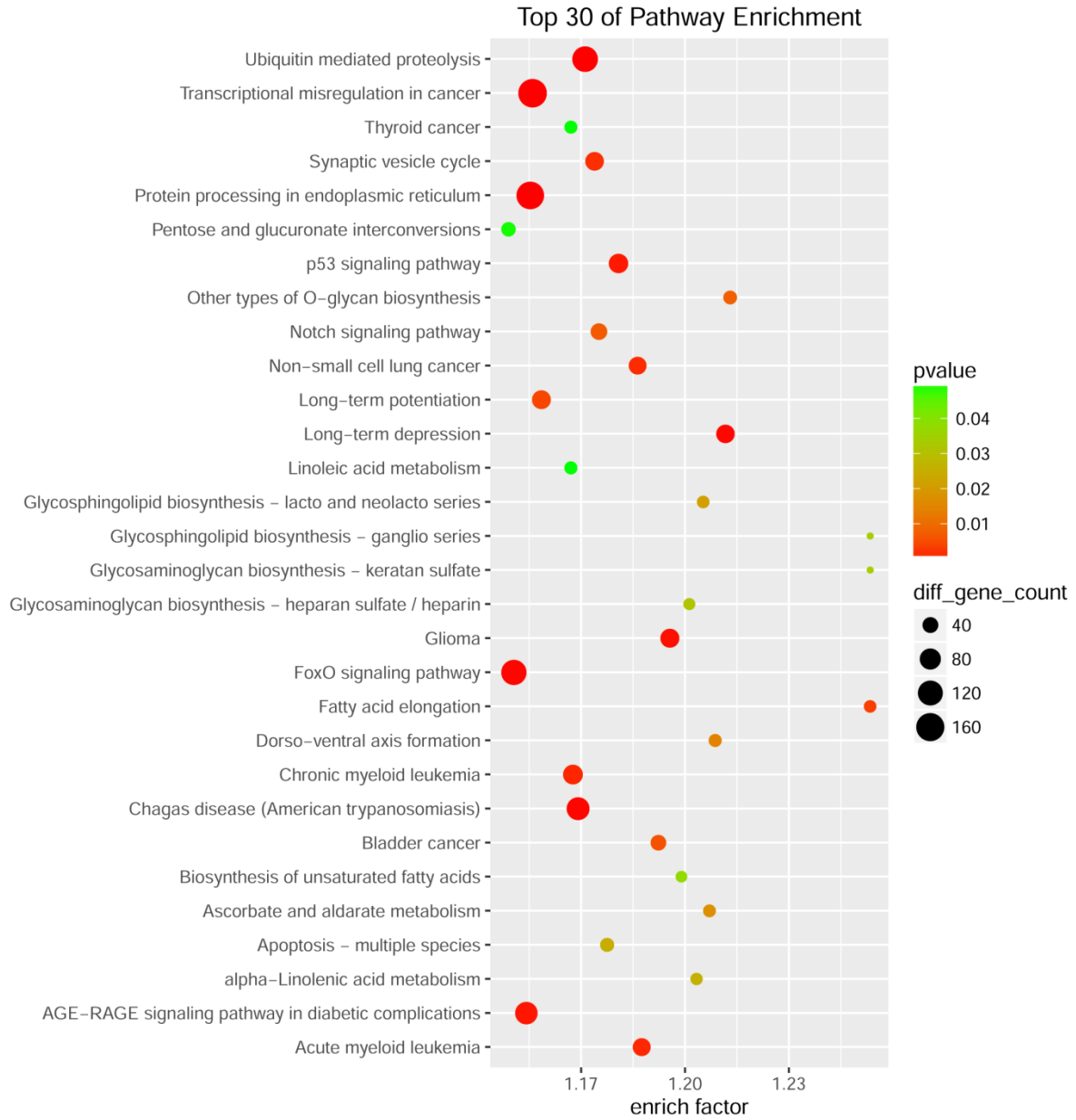
**A.** Decreased expression of GLUT-1 in HCC cells by PDCM-GLUT-1. **B.** Decreased expression of CA9 in HCC cells by PDCM-CA9. **C.** Decreased expression of miR-21 in HCC cells by PDCM-miRNA-21. **D.** Decreased expression of miR-10 in HCC cells by PDCM-miR-10b. Experiments were performed in triplicate. \*,  $P < 0.05$ . \*\*,  $P < 0.01$ . PDCM-CA9, CA9 siRNA was encapsulated in PDCM nano-particles. PDCM-miR-21, miR-21 siRNA were encapsulated in PDCM nano-particles.



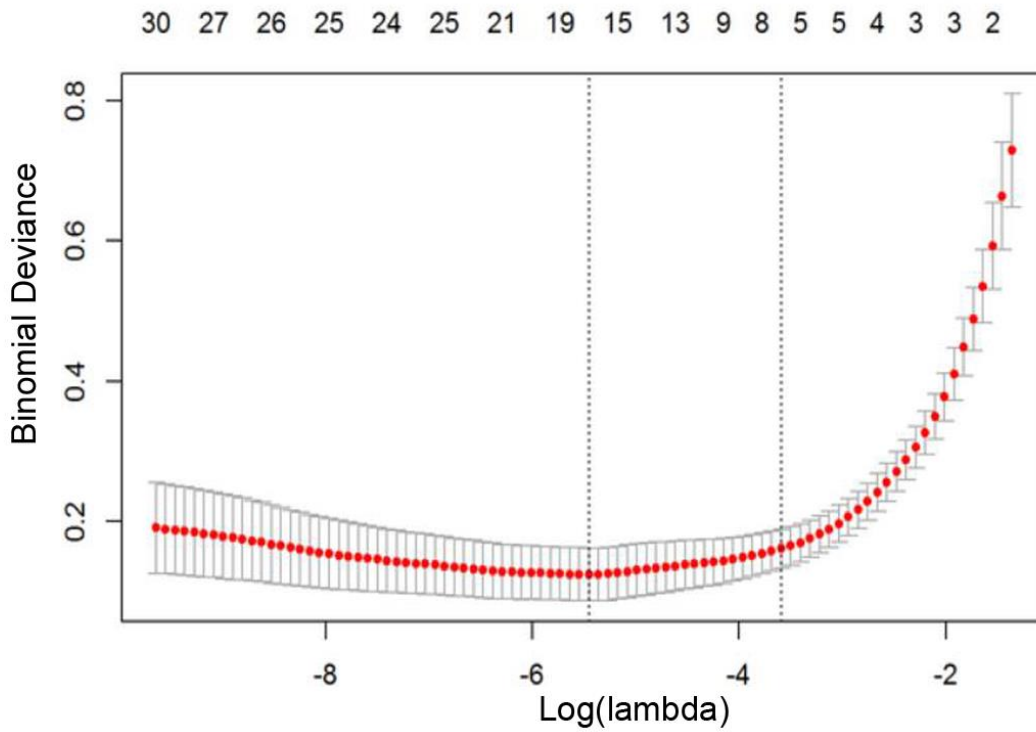
**Supplementary Figure S6. Proliferation of recipient cells treated with different exosomes assessed by MTT assays at 12h, 24h, 36h, 48h, and 60h.** Non-Ac exo, exosomes derived from HCC cells cultured in the non-acidic medium. Ac mock exo, exosomes derived from HCC cells cultured in an acidic medium. Ac ctrl shRNA exo, exosomes derived from HCC cells transfected with empty vector cultured in an acidic medium. HIF-1 KD exo, exosomes derived from HIF-1 $\alpha$  KD HCC cells. HIF-2 KD exo, exosomes derived from HIF-2 $\alpha$  KD HCC cells. HIF-1+2 KD exo, exosomes derived from HIF-1 $\alpha$  and HIF-2 $\alpha$  KD HCC cells. \*,  $P < 0.05$ .



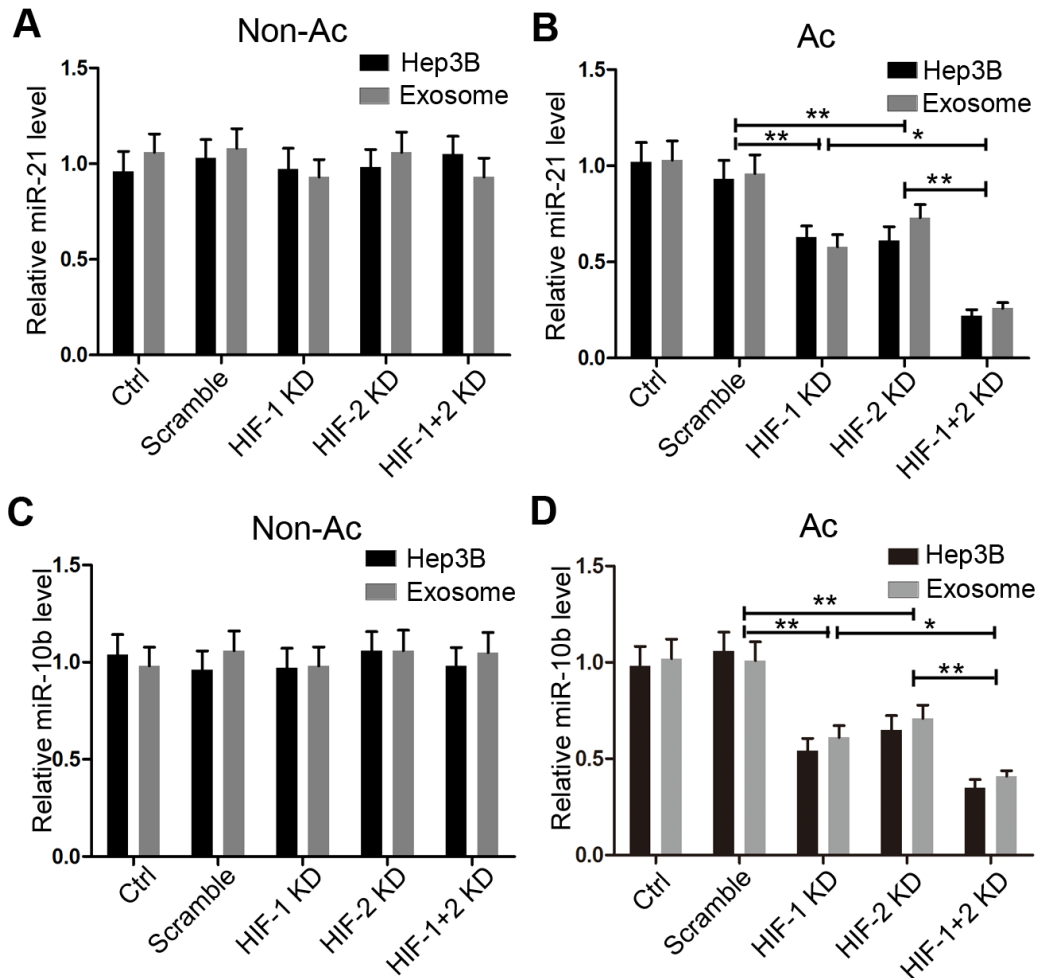
**Supplementary Figure S7. The 30 top GO enrichments in 81 different miRNAs between acidic and non-acidic exosomes analyzed by miRNA microarray.**



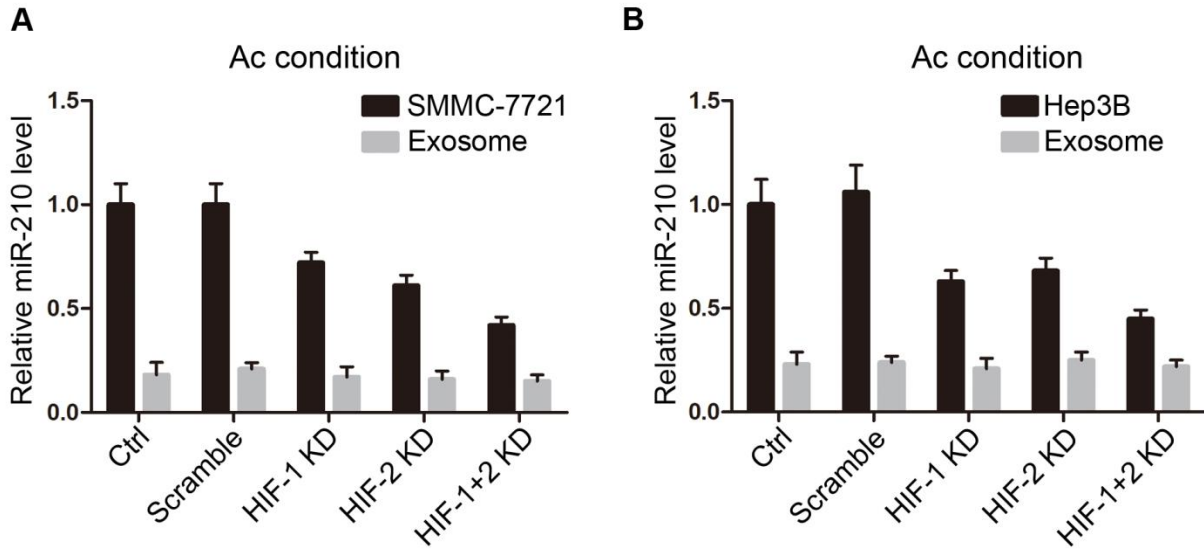
**Supplementary Figure S8. The 30 top KEGG pathways enrichment in 81 different miRNAs between acidic and non-acidic exosomes analyzed by miRNA microarray.**



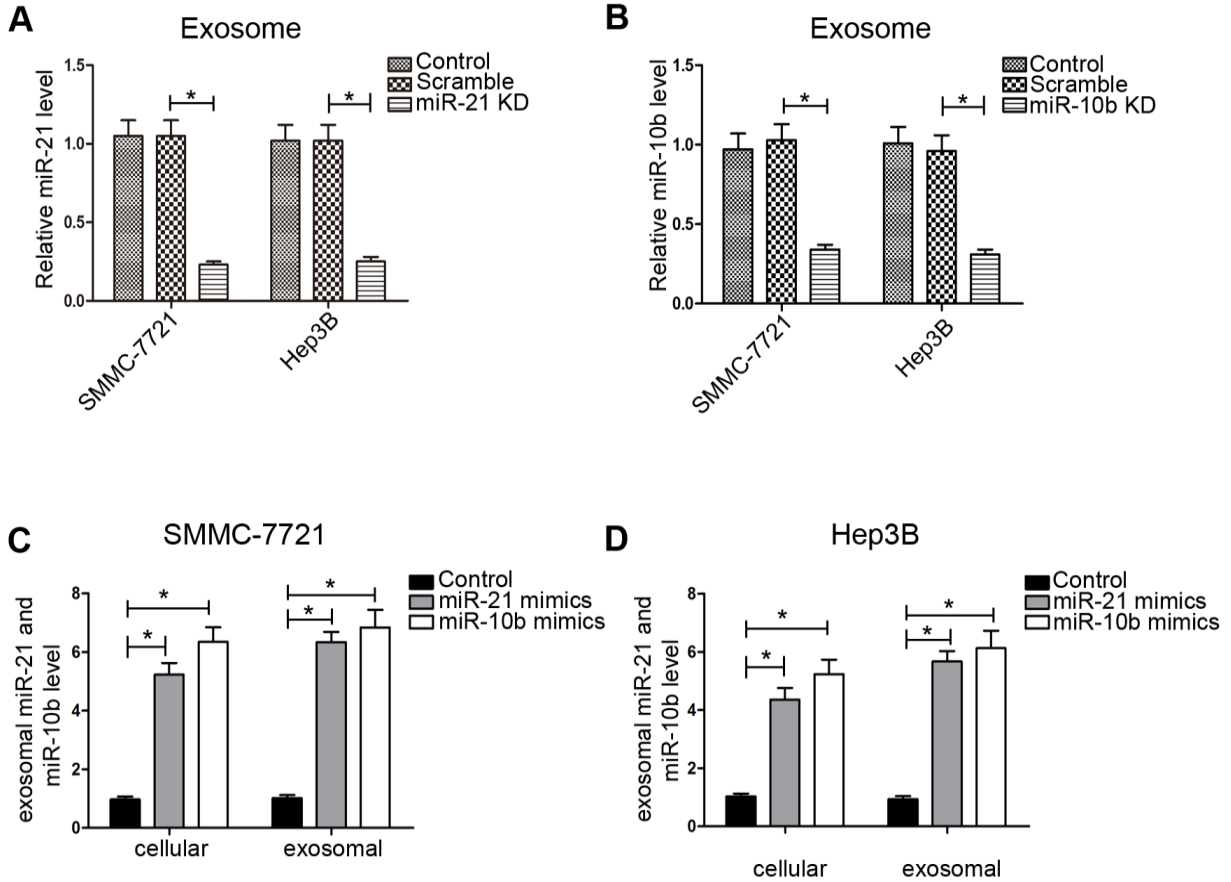
**Supplementary Figure S9. Ten-time cross-validation for tuning parameter selection in the LASSO model by using TCGA HCC dataset.** The dotted vertical lines are drawn at the optimal values by minimum criteria and 1-SE criteria. We plotted the partial likelihood deviance versus  $\log(\lambda)$ , where is the tuning parameter.



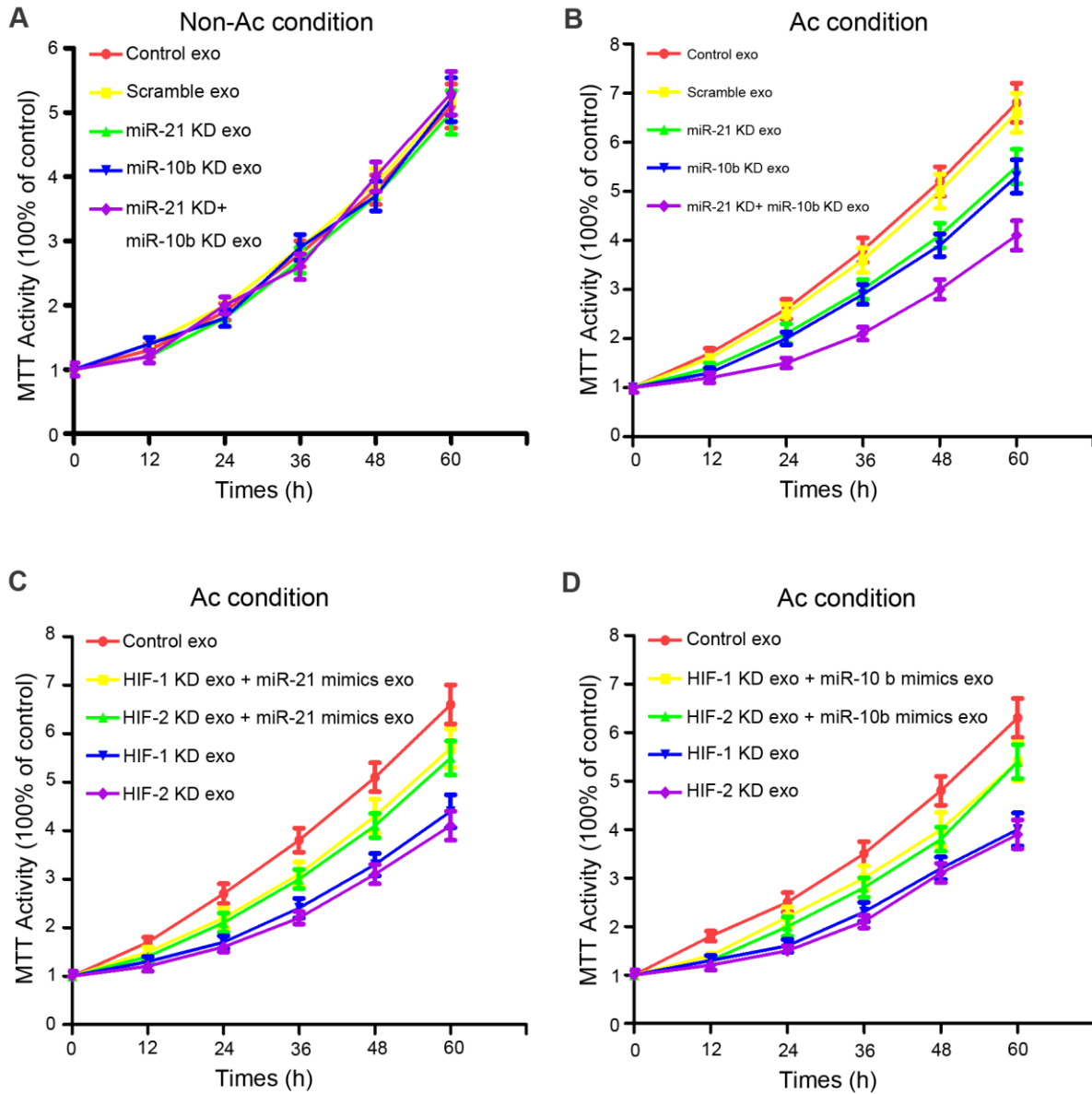
**Supplementary Figure S10. Acidic pH stimulates cellular and exosomal miR-21 and miR-10b expression in a HIF-1 $\alpha$  or HIF-2 $\alpha$ -dependent manner in hep3B cell lines. A and C.** In non-acidic conditions, cellular and exosomal miR-21 and miR-10b levels were not significantly affected by either HIF-1 $\alpha$  or HIF-2 $\alpha$  knockdown. **B and D.** In acidic conditions, cellular and exosomal miR-21 and miR-10b levels were significantly decreased by HIF-1 $\alpha$  or HIF-2 $\alpha$  knockdown. Experiments were performed in triplicate. \*,  $P < 0.05$ . \*\*,  $P < 0.01$ . HIF-1 KD, HIF-1 $\alpha$  KD Hep3B cells. HIF-2 KD exo, HIF-2 $\alpha$  KD Hep3B cells. HIF-1+2 KD exo, HIF-1 $\alpha$  and HIF-2 $\alpha$  KD Hep3B cells. \*,  $P < 0.05$ .



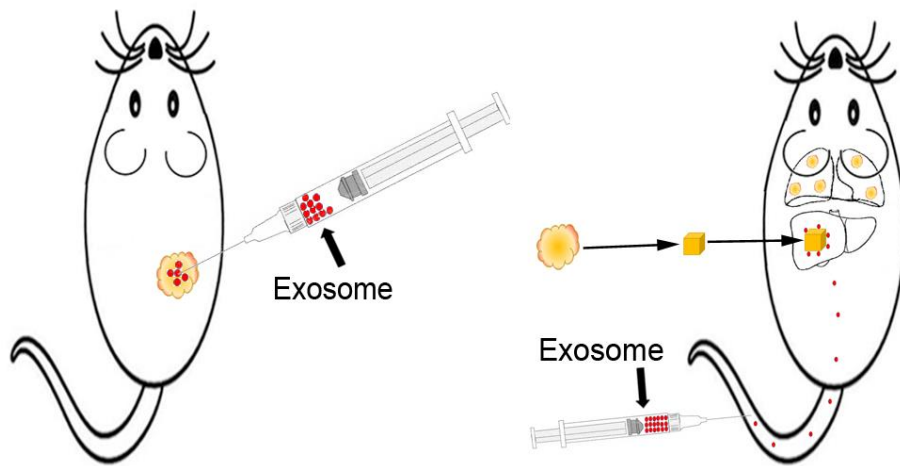
**Supplementary Figure S11.** The level of cellular miR-210 (another target of HIF-1 $\alpha$ ) in HCC cell line was significantly decreased, whereas the level of exosomal miR-210 was not altered after silencing of HIF-1 $\alpha$  and/or HIF-2 $\alpha$  in SMMC-7721 and Hep3B cell lines under pH 6.6 condition.



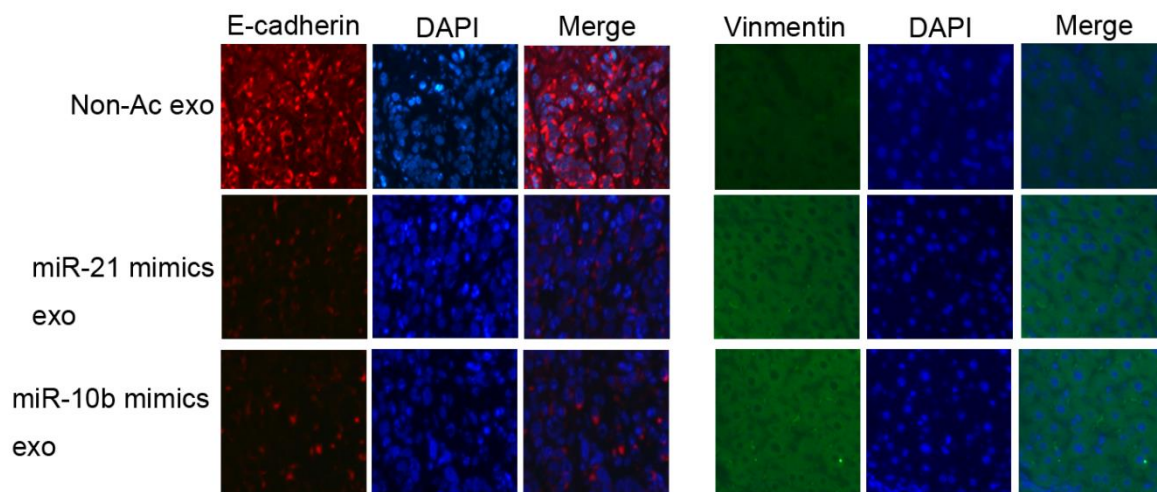
**Supplementary Figure S12. Cell proliferation by MTT assay. A and B.** Exosomes derived from miR-21 and miR-10b KD cells cultured in acidic condition decrease the proliferation of recipient cells. **C and D.** The expression of miR-21 and miR-10b mimics in HIF-1 $\alpha$  or HIF-2 $\alpha$  KD cells increase the proliferation of recipient cells. Experiments were performed in triplicate. \*,  $P < 0.05$ . miR-21 KD exo, exosome derived from miR-21KD HCC cells. miR-10b KD exo, exosome derived from miR-10b KD HCC cells. miR-21 mimics exo, exosome derived from miR-21 mimics HCC cells. miR-10b mimics exo, exosome derived from miR-21 mimics HCC cells.



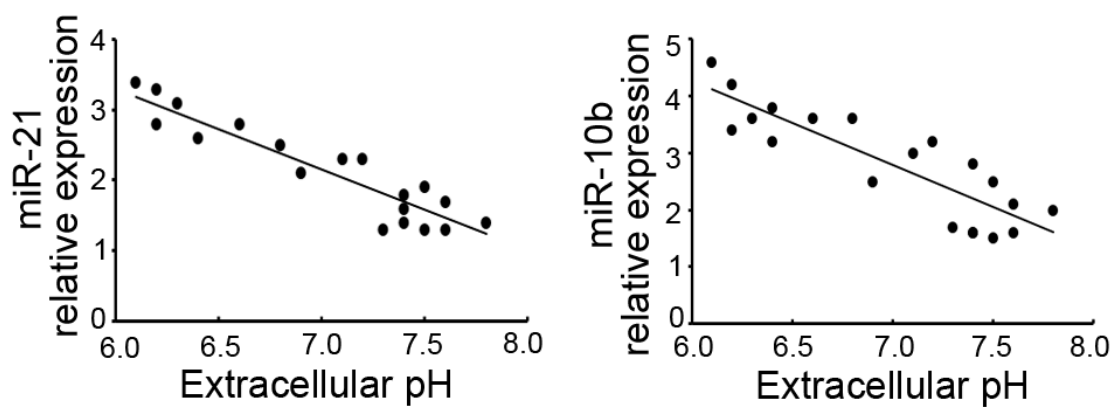
**Supplementary Figure S13. Expression of miR-21 and miR-10b regulated by cellular miR-21 and miR-10b in HCC cells. A and B.** Knockdown cellular miR-21 and miR-10b decreased exosomal miR-21 and miR-10b expression. **C and D.** Exosomal miR-21 and miR-10b expression was increased by miR-21 and miR-10b mimics in HCC cell line. Experiments were performed in triplicate. \*,  $P < 0.05$ . miR-21 KD, miR-21KD HCC cells. miR-10b KD, miR-10b KD HCC cells. miR-21 mimics, miR-21 mimics HCC cells. miR-10b mimics, miR-21 mimics HCC cells.



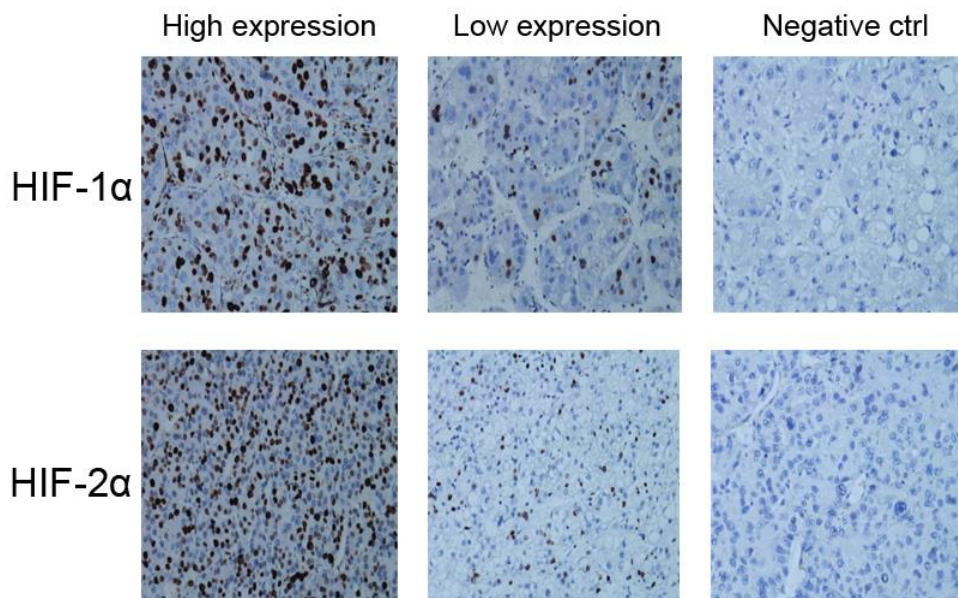
**Supplementary Figure S14. The xenograft model.** SMMC-7721 cells were injected into the flanks of BALB/C-nu/nu athymic nude mice. After 2 weeks, the subcutaneous tumors were resected into 1 mm<sup>3</sup> cubes, which were then implanted into the left lobes of the livers of the nude mice. Exosomes (three times a week, 1 µg/g for each time) were applied in an *in vivo* assay. At day 50, the liver and lung were dissected, fixed by formalin, and stained with haematoxylin & eosin. Consecutive tissue sections were used to examine the metastatic nodules in the lung and counted under a microscope.



**Supplementary Figure S15. Immunofluorescence stain shows the expression of E-cadherin and Vimentin in xenograft tumors.** Non-Ac exo, exosome derived from non-acidic microenvironment culture in HCC cells. miR-21 mimics exo, exosome derived from miR-21 mimics HCC cells. miR-10b mimics exo, exosome derived from miR-21 mimics HCC cells.



Supplementary Figure S16. Correlation of exosomal miR-21 and miR-10b and extracellular pH in 20 E-HCC patients' fresh tissues.



**Supplementary Figure S17. Immunohistochemical stain shows the expression of HIF-1 $\alpha$  or HIF-2 $\alpha$  in 124 E-HCC paraffin-embedded tissues.**